Preparation and Characterization of Venlafaxine Hydrochloride-Loaded Chitosan Nanoparticles and *In Vitro* Release of Drug

Sunil Shah,[1] Angshuman Pal,[1] V. K. Kaushik,[2] Surekha Devi[1]

[1]*Department of Chemistry, Faculty of Science, The Maharaja Sayajirao University of Baroda, Vadodara 390002, India*
[2]*Research and Development Centre, Reliance Industries Limited, Vadodara Manufacturing Division, Vadodara 391934, India*

Received 27 September 2007; accepted 24 November 2008
DOI 10.1002/app.29807
Published online 24 February 2009 in Wiley InterScience (www.interscience.wiley.com).

ABSTRACT: The venlafaxine hydrochloride (VHL)-loaded chitosan nanoparticles were prepared by ionic gelation of chitosan (CS) using tripolyphosphate (TPP). The nanoparticles were characterized using FTIR, differential scanning calorimetry, X-ray diffraction, dynamic light scattering, transmission electron microscopy, and X-ray photoelectron spectroscopy. The effect of concentration of CS, polyethylene glycol (PEG), VHL and CS/TPP mass ratio on the particle size and zeta potential of nanoparticles was examined. The particle size of CS/TPP nanoparticles and VHL-loaded CS/TPP nanoparticles was within the range of 200–400 nm with positive surface charge. In the case of VHL-loaded nanoparticles and PEG-coated CS/TPP nanoparticles, the particle size increases and surface charge decreases with increasing concentration of VHL and PEG. Both placebo and VHL-loaded CS/TPP nanoparticles were observed to be spherical in nature. PEG coating on the surface of CS/TPP nanoparticles was confirmed by XPS analysis. Maximum drug entrapment efficiency (70%) was observed at 0.6 mg/mL drug concentration. *In vitro* drug release study at 37°C ± 0.5°C and pH 7.4 exhibited initial burst release followed by a steady release. © 2009 Wiley Periodicals, Inc. J Appl Polym Sci 112: 2876–2887, 2009

Key words: chitosan; nanoparticles; venlafaxine hydrochloride; ionic gelation

INTRODUCTION

In the last decade, several synthetic and natural polymers have been examined for pharmaceutical applications. Among the natural polymers chitosan (CS) is the second abundant polysaccharide and cationic polyelectrolyte, comprising copolymers of glucosamine and *N*-acetyl glucosamine linked by β-(1–4) linkages. It can be prepared by partial deacylation of acetamido group of chitin side chain by strong alkaline solution. CS is nontoxic, hydrophilic, biocompatible, and because of its cationic nature, has very good mucoadhesive, antibacterial, and membrane permeability properties.[1] Because of the presence of free hydroxyl and amino groups, it can strongly bind to negatively charged surfaces of cell, mucus or other negatively charged polymers through electrostatic or hydrogen bonding and can also be chemically modified to suit for enzyme immobilization,[2] separation media,[3] protein adsorption,[4] absorbable sutures,[5] food and nutrition,[6] photography,[7] and in controlled release drug delivery systems in various forms.[8–12]

A variety of CS-based colloidal delivery systems have been reported for the delivery of polar drugs, peptides, proteins, vaccines, and DNA.[13–16] Drugs that have successfully transported into the brain using nanoparticulate drug carrier systems include doxorubicin, lopramide, tubocurarine, dipeptide kytorphin, haxapeptide dalargin, and the NMDA receptor antagonist.[17,18] Various methods such as emulsion crosslinking,[19,20] ionotropic gelation,[21,22] emulsification/solvent evaporation,[23] spray drying,[24] and coacervation/precipitation[25,26] have been adopted to prepare the CS/TPP nanoparticles. CS micro/nanoparticles are mainly prepared by chemical crosslinking of linear chains of chitosan with suitable bifunctional crosslinking agent such as glutaraldehyde or ethylene glycol diglycidyl ether, which generally reduce solubility, increase resistance to chemical degradation but impart physiological toxicity in the system. An alternative route to overcome the toxicity level is through intermolecular or intramolecular linkages between positively charged quaternary amine from CS in acidic medium and negatively charged multivalent counter ion like TPP[27] without using crosslinkers. Bodmeier et al.[28] were the first to report the ionotropic gelation of CS

Correspondence to: S. Devi (surekha_devi@yahoo.com).
Contract grant sponsors: GUJCOST (Gandhinagar, Gujarat).

with TPP for drug encapsulation. Subsequently, increase in research in the preparation of CS nanocarriers for successful delivery of small drugs, proteins and genes is reflected in the increased number of published articles in this field. Desai et al.[29] reported that the particle uptake by caco-2 cell lines depends significantly upon the particle's diameter. They have observed that particles of 100-nm size have 2.5-fold greater uptake on the weight basis than the 1-μm size particles. Particle size dependent performance was also reported by Gref et al.[30] for polyethylene oxide-polylactic acid nanospheres, where it was observed that the rapid clearance of these nanospheres from the blood stream is avoided. More recently, hydrophilic nanoparticles based on CS have received increasing attention due to their capacity to cross the biological barrier by protecting the entrapped drug. Hydrophobic character of CS was altered through blending, grafting, and chemical modification using polyvinyl alcohol, polyvinyl pyrolidone and polyethylene glycol and its derivatives. Zhang et al.[31] achieved enhancement in nasal absorption of insulin through PEG grafted CS/TPP nanoparticles of varying sizes synthesized through ionic gelation technique. Calvo et al.[32] could succeed in developing chitosan/polyethylene oxide nanoparticles with 80% entrapment of bovine serum albumin for controlled release of protein from the nanoparticles. Wu et al.[33] have reported initial burst followed by an extended release of ammonium glycyrrhizinate encapsulated in CS/TPP Nanoparticles. They have also reported that addition of PEG to CS decreases the encapsulation efficiency and surface charge on nanoparticles. Gupta and Ravikumar[34] succeeded in synthesizing pH-responsive CS/PEG microspheres by vapor phase crosslinking technique with 93% isoniazide entrapment and observed a near zero order release kinetics. Sugimoto et al.,[35] Mo et al.[36] and Tokura et al.[37] used PEG derivatives to modify CS which was used in the preparation of nanoparticles through ionotropic complexation. VHL is highly soluble in water and due to very short steady state elimination half-life (3–4 h),[38,39] it is very difficult to develop a pharmaceutical formulation with a slow dissolution rate of freely soluble drug. Hence to keep a stable therapeutic level, multiple daily administrations of VHL based formulations are needed. Both the immediate and extended release formulation have efficacy in reducing symptoms of depression. However, the extended release formulation has advantages in increasing patient compliance. Besides from the marketed formulations, many researchers have tried to prepare controlled release formulation of VHL. Yang and Lopina[40] developed extended release formulation of VHL based on polyamidoamine dendrimers and reported that, the drug was released in a sustained way and almost half of the conjugated drug was released within 18 h. They also correlate the effect of percentage loading on burst release. They have reported 92% release from 75 mg VHL-loaded matrix, whereas only 50% release from 8 mg VHL-loaded matrix. Use of polyvinylpyrollidone and cellulose derivatives for the encapsulation of VHL is reported in patent forms.[41,42]

CS/TPP nanoparticles prepared by different preparation protocols have been in recent years widely studied carriers for various pharmaceutically active ingredients with varying degree of effectiveness and drawbacks. The aim of the present work is to further explore the ionic complexation process for the preparation of CS micro/nanoparticles for the incorporation of model drug VHL and subsequent study of *in vitro* release of VHL from the nanoparticles. Optimization of the fabrication parameters was done to achieve maximum encapsulation efficiency and controlled release of VHL from CS/TPP nanoparticles.

MATERIALS AND METHODS

Materials

VHL (99.9%) was obtained as a gift sample from Alembic Chemicals (Baroda, India). CS derived from crab shell, in the form of fibrils flakes was obtained from Sigma-Aldrich (Stingham, Germany). The degree of deacylation of CS determined by FTIR analysis observed to be 82.5%. TPP was purchased from Sulab Chemicals (Baroda, India). PEG (M_n = 4000 units) was obtained from Merck (Mumbai, India). All other reagents used were of analytical grade.

Preparation of CS and VHL-loaded CS/TPP nanoparticles

CS/TPP nanoparticles were prepared according to the procedure reported by Calvo et al.[32] based on the ionic gelation of CS with TPP anions. Ionotropic gelation takes place when the positively charged quaternary amine groups in CS interact with the negatively charged TPP. CS solution (1% w/v) was prepared by dissolving 1 g of CS in 100 mL of 1% v/v acetic acid under magnetic stirring at room temperature for 20–24 h. The solution was filtered through 0.2-μm nylon filter before use. TPP solution of 0.05% w/v was prepared by dissolving 0.5 g of TPP in 1 L of distilled deionized water. Addition of variable volumes of TPP solution to 4 mL of the CS solution in 200 μL increments lead into spontaneous formation of nanoparticles at room temperature under magnetic stirring.

For the preparation of VHL-loaded CS/TPP nanoparticles, different concentrations of VHL (0.2, 0.4,

0.6, 0.8, 1.0 mg/mL) were added to CS solution (0.15% w/v) and gently mixed for 1 h under mild stirring before the addition of TPP solution (0.05% w/v).

PEG-coated CS/TPP nanoparticles were prepared by adding TPP (0.05% w/v) solution to CS solution (0.15% w/v) containing various amounts of PEG (10.0–50.0 mg/mL).

Characterization of nanoparticles

The morphology, size, and shape of the placebo and VHL-loaded CS/TPP nanoparticles were examined by using transmission electron microscope (CM 120, Philips, Eindhoven, Netherlands) at accelerating voltage of 200 kV. One drop of suspension of the prepared nanoparticles was placed on 300 mesh carbon-coated copper grid. The grid was dried under IR lamp and the images of representative areas were taken at suitable magnifications.

A Brookhaven's 90 plus dynamic light scattering equipment with a solid state laser source operated at 688 nm was used to measure the particle size and size distribution of freshly prepared CS/TPP nanoparticles and drug-loaded CS/TPP nanoparticles in a dynamic mode. The scattering intensities from the samples were measured at 90° using photomultiplier tube. Average hydrodynamic radius of latex particles (R_h) was calculated from the intrinsic diffusion coefficient (Do) as

$$R_h = KT/(6\pi\eta D_0) \quad (1)$$

where K is a Boltzmann constant, T is the absolute temperature and η is the viscosity of the dispersing medium. The polydispersity index (PI), which is the variance of the size distribution, was obtained with the PSDW 32 bit software provided with the instrument.

The zeta potential of the nanoparticles was measured using same instrument after calibration with BI-ZR_3. Samples were diluted 10–100 times with 0.1 mM KCl and placed in the electrophoretic cell where a potential of ±150 mV was applied.

CS/TPP nanoparticles were collected by centrifugation at 15,000 rpm for 30 min at room temperature. Supernatant solution was discarded and nanoparticles were resuspended in double distilled deionized water and then lyophilized for a period of 24 h to get dry nanoparticles.

FTIR spectra of CS, VHL, placebo nanoparticles, VHL-loaded CS/TPP nanoparticles and PEG-coated CS/TPP nanoparticles were recorded on a Perkin–Elmer Rx_1 FTIR spectrophotometer (Massachusetts) using 1-cm diameter KBr pellets.

Differential scanning calorimetric (DSC) analysis was carried out using a Mettler-Toledo 822 instrument. The instrument was calibrated using indium as a standard and samples were heated in sealed aluminum pans between 30 and 400°C at a heating rate of 10°C/min.

Powder X-ray diffraction (XRD) patterns for CS, PEG, VHL, placebo nanoparticles, VHL-loaded CS/TPP nanoparticles and PEG-coated CS/TPP nanoparticles were recorded on a Philips X'pert multipurpose diffreactometer (MPD range, Germany) using a Ni-filtered Cu Kα radiation over the 2θ range of 3–100°.

X-ray photoelectron spectroscopy (XPS) analysis was carried out using VG Scientific ESCALAB MK II spectrometer equipped with Aluminum–Pottasium (Al/Mg) twin anode. Survey scan and multiscan quantitative data were collected using Al-K source at 50 eV analyzer pass energy and high resolution data was collected using 20 eV pass energy. Vacuum in the analysis chamber was maintained at better than 10^{-8} mbar throughout XPS experiments. The spectrometer was calibrated using Ag (3 $d_{5/2}$) photoelectron line of silver.[43] The C (1S) photoelectron line from neutral carbon at 285 eV was used as internal reference in binding energy measurements. Binding energy measurements were accurate to ±0.1 eV and are average of two experiments. Data was analyzed on DELL computer interfacing the spectrometer.

Drug encapsulation efficiency of nanoparticles

The drug encapsulation efficiency was determined by separating the nanoparticles from the aqueous medium containing free VHL by centrifugation at 25,000 rpm, at 20°C for 30 min. The amount of free drug in supernatant was quantified by measuring absorbance at 274 nm using Perkin–Elmer Lambda 35 UV spectrophotometer and using appropriate calibration plot. The VHL encapsulation efficiency (EE) of the nanoparticles was calculated as follows:

$$\text{EE} = \frac{\text{Total VHL concentration} - \text{Free VHL concentration}}{\text{Total VHL concentration}} \quad (2)$$

All measurements were performed in triplicate and observed to be highly precise. The observed % relative error in the determination of drug encapsulation efficiency was less than 3.5% for triplicate measurements.

In vitro release

In vitro release study was performed according to the procedure reported by Hu et al.[44] *In vitro* release of VHL from CS/TPP nanoparticles was studied by

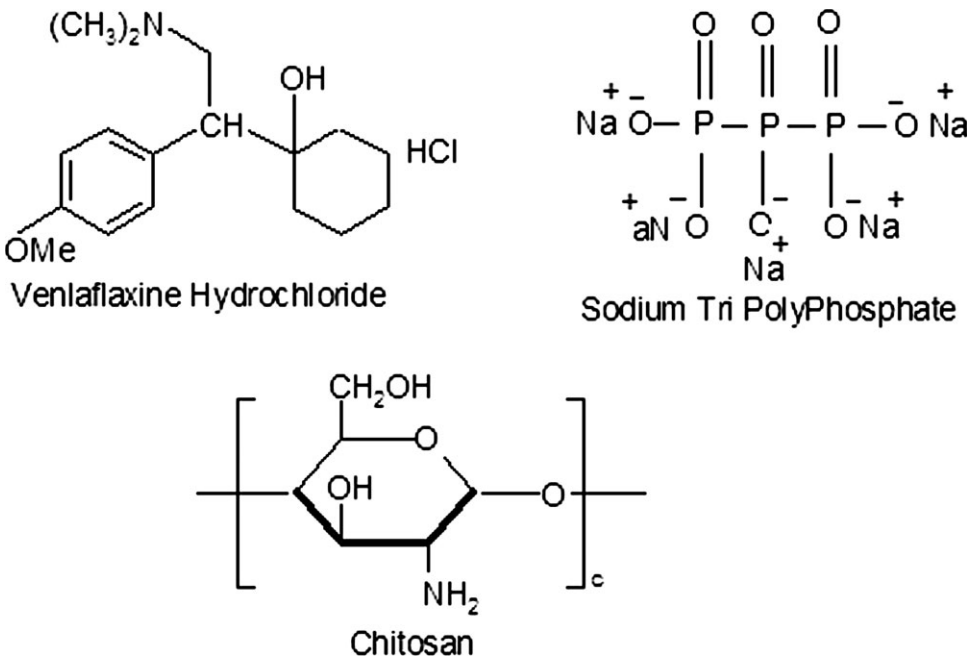

Figure 1 Chemical structure of (A) VHL, (B) TPP, and (C) CS.

redispersing separated nanoparticles (10 mg) in 2.5 mL freshly prepared phosphate buffer of 7.4 pH, in a dialysis membrane bag with molecular weight cut off at 5 kDa. The dialysis bag was placed in 50 mL of phosphate buffer of pH 7.4. The entire system was kept under magnetic stirring. Four milliliter of the release medium was removed and was replaced by fresh buffer solution at regular time intervals. The amount of drug in the released medium was evaluated from the absorbance measured at 274 nm. All the release studies were conducted in triplicate and mean values were taken.

RESULTS AND DISCUSSION

Characterization of CS/TPP nanoparticles

In the present study, we adapted the method of Calvo et al.[32] for the preparation of nanoparticulate system made of solely hydrophilic polymers. Nanoparticles were prepared by coacervation, which is a spontaneous phase separation process arising from electrostatic interaction, when oppositely charged macromolecules are mixed together. The success of the process is largely dependent on intermolecular linkages created between the negatively charged groups of TPP with that of positively charged amino groups of CS. A similar principle has been used by other research groups for the preparation of nanoparticles useful in the encapsulation and controlled release of peptides,[45] proteins,[46] and insulin.[47] As far as our knowledge, this is the first report for encapsulation of VHL in CS/TPP nanoparticles. The molecular structures of VHL, TPP, and CS are given in Figure 1.

The nature of interaction between the drug and CS or TPP was established through FTIR spectrometry. In the slightly acidic medium at pH 5, where nanoparticle formation takes place, VHL will be positively charged because of the presence of tertiary amino groups in its molecular structure (Fig. 1). Hence, during CS nanoparticle formation, besides hydrogen bonding, electrostatic interactions between TPP and drug molecules can take place. Figure 2 shows FTIR spectra of CS, CS/TPP nanoparticles, VHL, VHL-loaded CS/TPP nanoparticles, and PEG-coated CS nanoprticles. Three characteristics vibrational absorption bands observed in Figure 2(B) at 3445, 1610, and 1325 cm^{-1}, are respectively, due to the hydroxyl, $-NH_2$ and C≡N groups present in CS. In the case of placebo CS/TPP nanoparticles, [Fig. 2(A)] observed broadening of the peak in the range of 3200–3500 cm^{-1}in comparison with CS [Fig. 2(B)] can be attributed to the possible intermolecular hydrogen bonding. The observed shift in $-NH_2$ bending vibration from 1610 to 1539 cm^{-1} and appearance of a new peak at 1630 cm^{-1} can be attributed to the linkages between phosphate groups of TPP with ammonium groups of CS in nanoparticles. Similar observation is reported earlier by Calvo et al.[32] These interactions reduce CS solubility and are responsible for micro/nanoparticles separation from the solution. The presence of P=O group is indicated by the appearance of a peak at 1163 cm^{-1}. In the case of VHL [Fig. 2(D)], appearance of absorption band at 3352 cm^{-1} corresponds to the

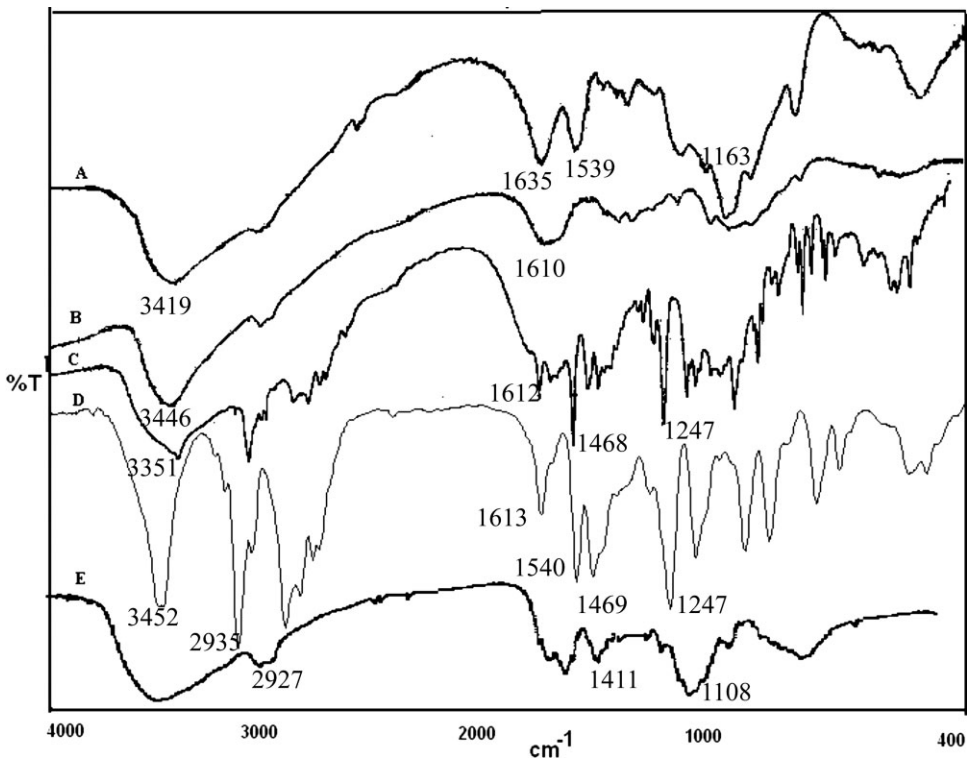

Figure 2 FTIR spectra of (A) CS/TPP nanoparticles, (B) CS, (C) VHL-loaded CS/TPP nanoparticles, (D) VHL, and (E) PEG-coated CS/TPP nanoparticles.

stretching vibrations of hydroxyl group and bands at 2935, 1515–1450, and 1247 cm^{-1} correspond to the stretching vibrations of aromatic CH, benzene ring, and methoxy group present in the drug structure. In the case of VHL-loaded CS/TPP nanoparticles [Fig. 2(C)], existence of characteristics bands at 2935, 1514–1469, 1247 due to venlafaxine hydrochloride and at 3352, 1612, and 1170 cm^{-1} due to hydroxyl, primary amino and P=O groups of chitosan nanoparticles indicate the presence of drug in CS/TPP nanoparticles. As shown in the FTIR spectrum of PEG-coated CS/TPP nanoparticles [Fig. 2(E)], characteristic absorption peaks at 2927, 1411, and 1108 cm^{-1} correspond to stretching and bending vibrations of $-CH_2$ group and presence of ether linkage respectively, providing a confirmation of incorporation of PEG in the nanoparticle matrix.

To confirm the physical state and interaction of the drug in the CS/TPP nanoparticles, the placebo nanoparticles, pure drug, physical mixture of the drug, and the placebo nanoparticles and VHL-loaded CS/TPP nanoparticles were examined by DSC, the results were given in Figure 3. This study revealed that placebo nanoparticles showed a broad endothermic peak at 124°C [Fig. 3(A)], whereas in the case of pure VHL [Fig. 3(B)], a sharp endothermic peak at 217°C corresponds to the melting point of VHL.[23] In the case of VHL-loaded CS/TPP nanoparticles [Fig. 3(C)], disappearance of the endothermic peak appearing at 217°C corresponding to melting point of the VHL indicates molecular level dispersion of drug in nanoparticle matrix, whereas, physical mixture of drug and nanoparticles [Fig. 3(D)] shows separate characteristic endothermic peaks for drug and nanoparticles. Similar results have also been reported earlier by Dhawan and Singla for Nifidipine-loaded chitosan microsphere.[48] Observed broad endothermic peak for CS/TPP nanoparticles at 124°C was shifted to 116°C [Fig. 3(E)] for PEG-coated CS/TPP nanoparticles. The observed decrease in the endothermic peak for PEG-coated CS/TPP nanoparticles supports interaction between CS and PEG.[33]

The X-ray diffraction patterns of VHL, CS, CS/TPP nanoparticles, and VHL-loaded CS/TPP nanoparticles are shown in Figure 4. XRD patterns of CS [Fig. 4(B)] showed two prominent crystalline peaks at 10.375° and 20.175°. In the case of CS/TPP nanoparticles [Fig. 4(C)], there was significant decrease in the intensity of characteristic peaks of chitosan, which is in agreement with the results reported by Wan et al.[49] The distinct differences in the diffraction patterns of CS and CS/TPP nanoparticles could be attributed to the modification in the arrangement of molecules in the crystal lattice. From the XRD patterns of VHL [Fig. 4(A)] and VHL-loaded CS/TPP nanoparticles [Fig. 4(D)], molecular level dispersion of VHL in CS/TPP nanoparticles is clearly indicated

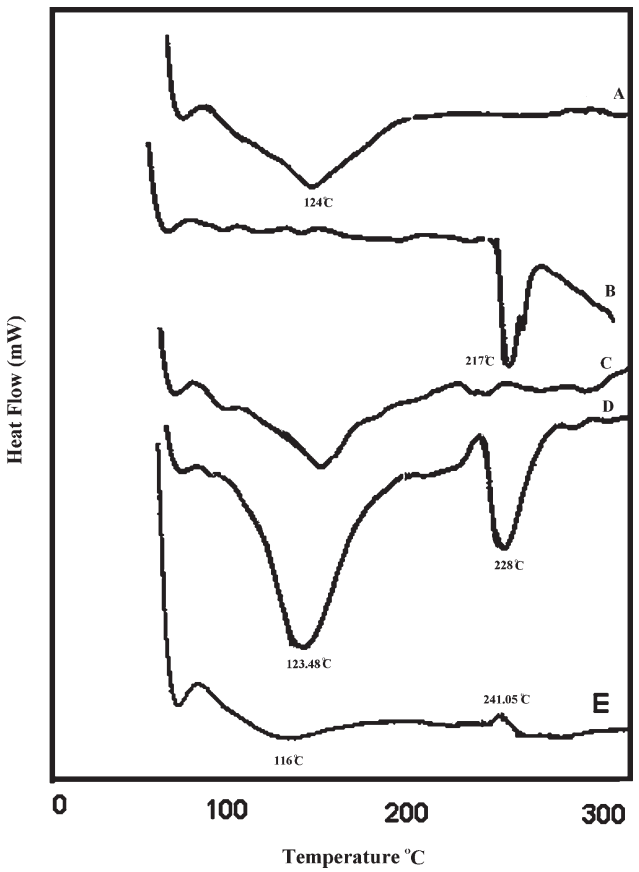

Figure 3 DSC thermograms of (A) CS/TPP nanoparticles, (B) VHL, (C) VHL-loaded CS/TPP nanoparticles, (D) physical mixture of VHL and placebo nanoparticles, and (E) PEG-coated CS/TPP nanoparticles.

from the disappearance of XRD bands of the drug appearing at $2\theta = 8.3$, 12.66, 13.49, 15.56, 20.32, 25.00, 28.48, and 35.56°. Sarmento et al.[50] in the study of dorzolamide and pramipexole in CS/TPP nanoparticles have also reported similar observation. From XRD data, they have suggested that, pramipexole probably forms a molecular level dispersion or an amorphous nanodispersion within the CS matrix of the nanoparticles. However, crystallization of Dorzolamide was reported during its entrapment in CS/TPP nanoparticles.

TEM images of plecebo nanoparticles and VHL-loaded CS/TPP nanoparticles are given in Figure 5. It was observed that TEM analysis of placebo CS/TPP nanoparticles exhibits spherical morphology with particle size of $\sim 250 \pm 15$ nm [Fig. 5(A)], whereas irregularity in shape and size (250–300 nm) was observed in the case of VHL-loaded CS/TPP nanoparticles [Fig. 5(B)]. The observed size of these nanoparticles from TEM analysis is in good agreements with the results obtained from dynamic light scattering studies.

Factors influencing the particle size, zeta potential, and encapsulation efficiency of CS/TPP nanoparticles

Effect of CS concentration and CS/TPP mass ratio

The physicochemical properties of nanoparticles are important in determining the physiological functions and stability of drug-loaded nanoparticles. The particle size is one of the most significant determinants in mucosal and epithelial tissue uptake and intracellular trafficking.[51] Surface charge is another important determinant in not only the stability, mucoadhesiveness, and permeation enhancing effects of nanoparticles[52,53] but also in the ability of nanoparticles to escape from the endolysosomes.[54] CS is a weak base polysaccharide, insoluble in neutral and alkaline medium. In acidic medium, positively charged quaternary amine group accelerates gelation with polyanion TPP, due to inter and intramolecular crosslinkages mediated by the polyanions. Though nanoparticles are formed instantaneously on mixing of TPP and CS solution, the size and zeta potential of the nanoparticles depend largely on the concentration of CS and TPP, CS/TPP mass ratio, molecular weight of CS, pH of the medium, and stirring rate. Mi et al.[55] have reported the detailed kinetics of CS/TPP complex formation and curing mechanism.

A preliminary screening of different concentration ratios of CS/TPP combinations showed that, mainly both polymer ratio and total polymer concentration influenced the formation of nanoparticles. To examine effect of CS concentration on nanoparticles formation, CS solutions of different concentrations ranging from 0.05 to 0.25% (w/v) in 1% acetic acid were reacted efficiently with 0.05% aqueous solution of TPP. Concentration of drug was kept constant at already optimized concentration of 600 μg/mL. Effect of concentration of CS and CS/TPP mass ratio on particle size, zeta potential, and encapsulation efficiency of nanoparticles is illustrated respectively, in Figure 6(A–D). At fixed CS/TPP mass ratio (5 : 1) and drug concentration 600 μg/mL, it was observed that with increasing concentration of CS, particle size increases but zeta potential decreases [Fig. 6(A)], while, as CS concentration increases, VHL encapsulation efficiency decreases from 74 to 58% [Fig. 6(C)]. Similar observation was reported earlier for encapsulation of bovine serum albumin in CS/TPP nanoparticles. The increased viscosity of medium with increasing concentration of CS may be responsible for reduction in encapsulation efficiency and increase in particle size. The highly viscous nature of the gelation medium reduces the ionic interaction of CS with TPP leading to increase in particle size and also hinders the transfer of the drug molecules leading to reduction in encapsulation efficiency.

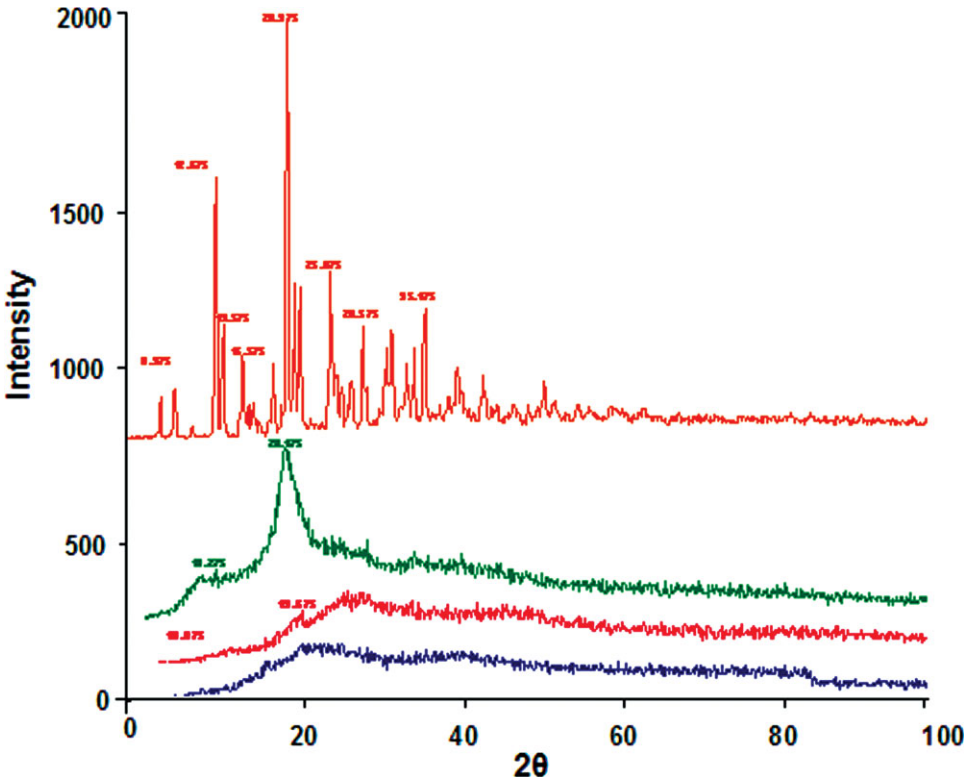

Figure 4 XRD patterns of (A) venlafaxine hydrochloride, (B) chitosan, (C) CS/TPP nanoparticles, and (D) venlafaxine hydrochloride-loaded CS/TPP nanoparticles. [Color figure can be viewed in the online issue, which is available at www.interscience.wiley.com.]

CS/TPP mass ratio is another important factor influencing the characteristics of the formed CS/TPP nanoparticles. To examine the effect of CS/TPP mass ratio on particle size, zeta potential, and encapsulation efficiency of VHL, nanoparticles were prepared as described earlier, at fixed concentration of CS (1.5 mg/mL). Variation in CS/TPP mass ratio from 3 : 1 to 7 : 1 showed increase in size and zeta potential of nanoparticles [Fig. 6(B)]. At fixed concentration of chitosan (1.5 mg/mL), with increase in the CS/TPP mass ratio, the pH of the solution increases due to increased TPP concentration favoring ionic interaction. Similar observation is reported earlier by Hu et al.[56] However, variation in CS/TPP mass ratio did not show any effect on the efficiency of VHL encapsulation [Fig. 6(D)]. Hence, these results provide an important link in manipulation and optimization of the particle size, surface charge, and also

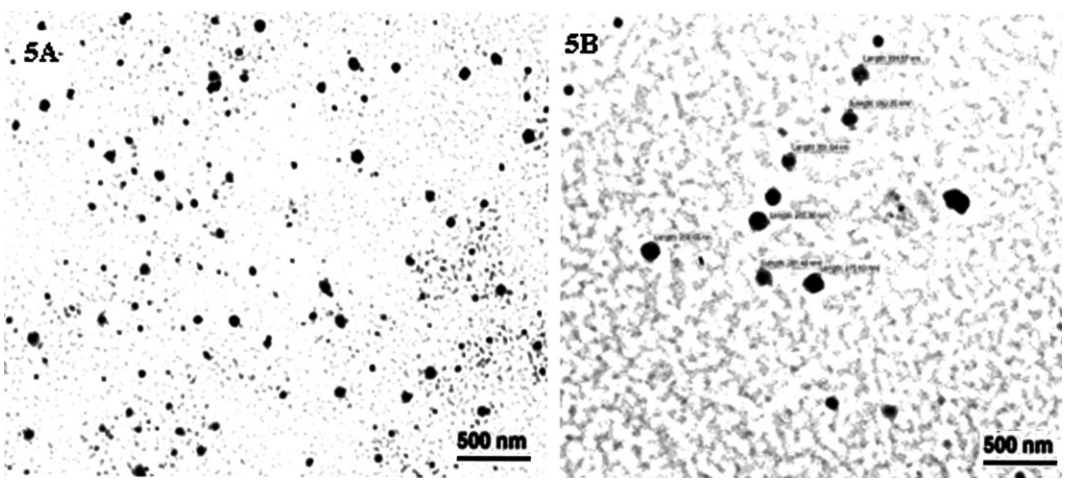

Figure 5 TEM image of (A) CS/TPP nanoparticles and (B) VHL-loaded CS/TPP nanoparticles. (CS = 0.15% w/v, TPP 0.05% w/v, VHL 0.6 mg/mL).

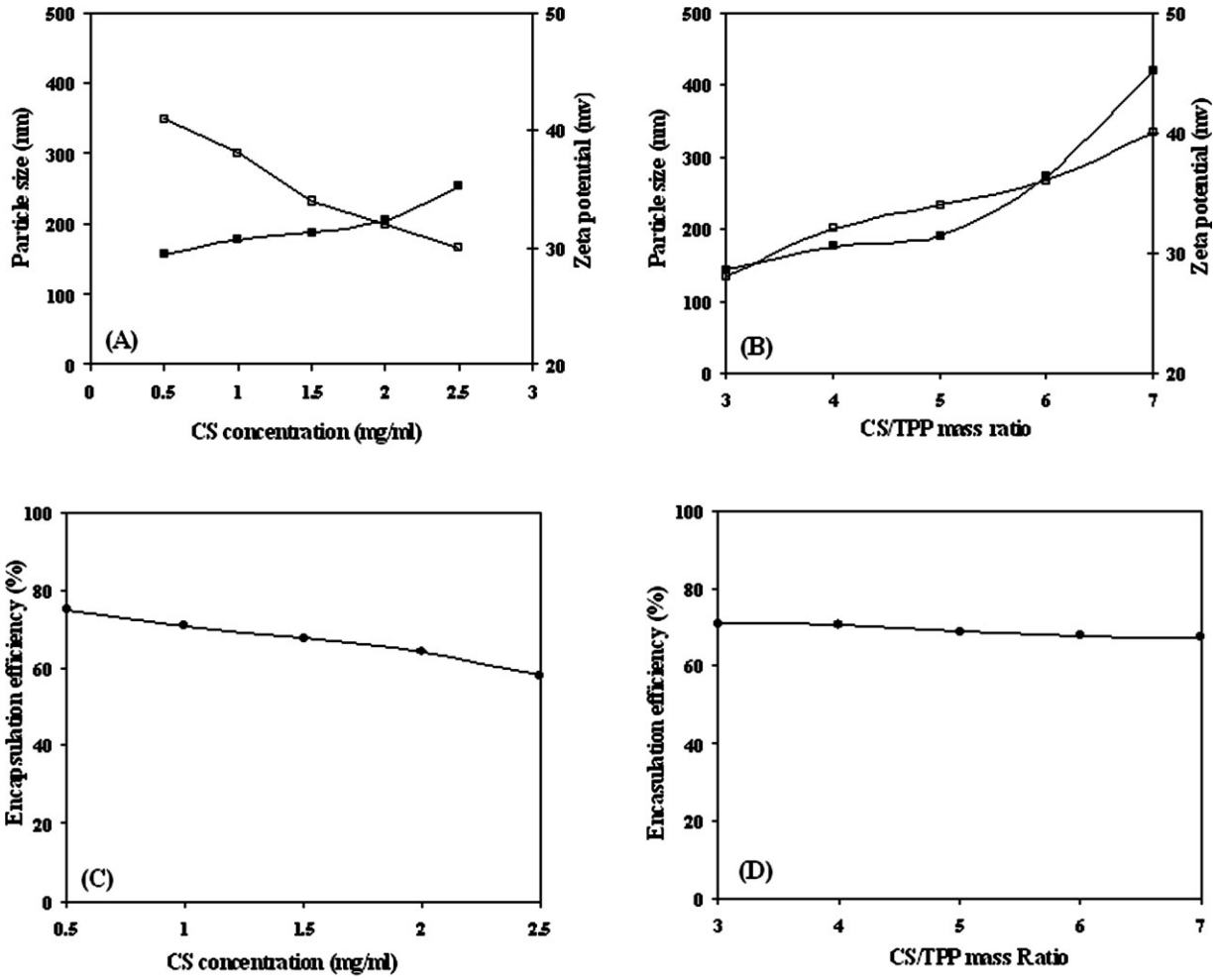

Figure 6 (A) Effect of CS concentration on (■) particle size and (□) zeta potential at CS-TPP mass ratio 5 : 1 and pH = 5. (B) Effect of CS/TPP mass ratio on (■) particle size and (□) zeta potential at pH = 5. (C) Effect of CS concentration on encapsulation efficiency at CS/TPP mass ratio 5 : 1 and pH = 5. (D) Effect of CS/TPP mass ratio on encapsulation efficiency at CS and VHL concentration 1.5 and 0.6 mg/mL at pH = 5.

encapsulation efficiency for projected applications. The observed % relative error in particle size measurements by DLS and % encapsulation efficiency was less than 3.5% and 4.1% respectively, for triplicate measurements.

Effect of VHL concentration

Figure 7(A,B) illustrate the effect of VHL concentration on entrapment efficiency, particle size, and zeta potential of nanoparticles at constant CS/TPP mass ratio of 5 : 1 at pH 5. As seen from Figure 7(A), with increase in drug concentration, encapsulation efficiency increases initially up to 600 μg/mL, and thereafter remains almost constant. Hence, further study was carried out at 600 μg/mL concentration. Figure 7(B) shows that the particle size of drug-loaded nanoparticles gradually increases and zeta potential decreases as the concentration of VHL increases from 0.2 to 1 mg/mL.

Effect of PEG incorporation

PEG is widely used as coating material in pharmaceuticals, due to its proven safety potential attributed by its hydrophilicity, nontoxicity, absence of antigenicity, and immunogenicity. Nanoparticles with the right coating can quickly slip through human mucus preventing the adherence of nanoparticles and viruses to the protein meshwork in the mucus, allowing them to become long circulating particles in physiological fluids. It was observed [Fig. 8(A)] that particle size increases and zeta potential decreases with no effect on encapsulation efficiency of VHL [Fig. 8(B)] with increase in PEG concentration. The increase in the size may be due to the intermolecular hydrogen bonding between the electropositive quaternary amine groups of CS with electronegative hydroxyl groups of PEG. Also, it is not surprising that the addition of PEG reduces the positive charge on the nanoparticles and hence nanoparticle suspension was observed to be stable

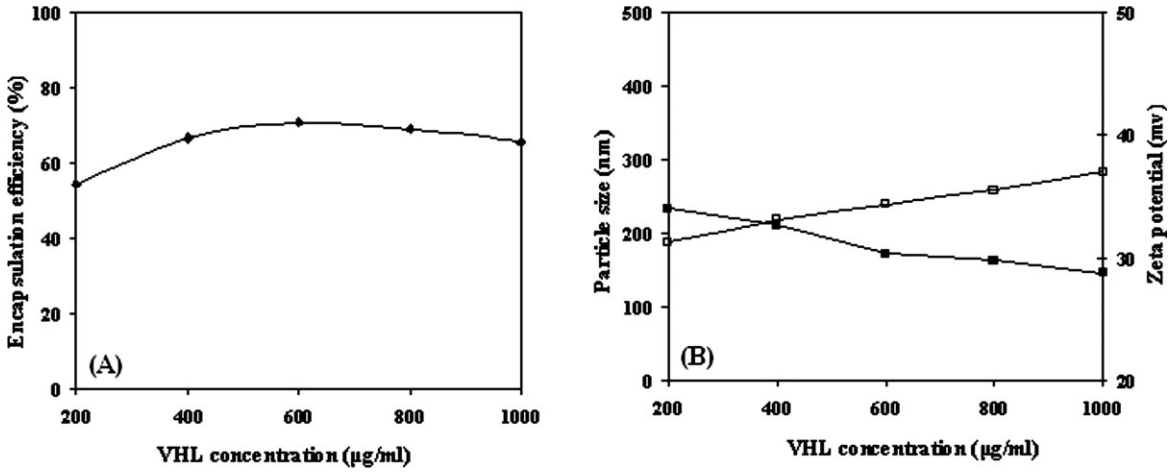

Figure 7 Effect of VHL concentration on (A) encapsulation efficiency and (B) particle size (■) and zeta potential (□). (CS/TPP mass ratio 5 : 1, pH = 5).

for a period of more than 6 months at room temperature (30 ± 1)°C. TEM image of PEG-coated CS/TPP nanoparticles is illustrated in Figure 9(A,B). Spherical particles with smooth and uniform coating on the surface were observed and the overall size of the particles was observed to be larger as compared to unmodified nanoparticles. To prove the coating on the surface of CS/TPP nanoparticles, XPS analysis was carried out. XPS survey scan of PEG and CS, indicated presence of C (1S) and O (1S) photoelectron lines for PEG and C (1S), N (1S) and O (1S) photoelectron lines for CS. As nitrogen photoelectron lines appear only in CS spectrum, presence of nitrogen and its quantitative comparison with carbon atoms was used as a probe for PEG coating on CS/TPP nanoparticles. Figure 10(A) shows XPS scan of CS/TPP nanoparticles and PEG-coated CS/TPP nanoparticles, wherein a decrease in the intensity of N (1S) has been noticed along with the increase in C (1S) and O (1S) photoelectron line intensities. Comparison of carbon and nitrogen content on the surface of CS/TPP nanoparticles and PEG-coated CS/TPP nanoparticles through XPS indicates increase in carbon concentration and considerable decrease in nitrogen content on the surface of PEG-coated sample compared to CS/TPP nanoparticles surface. These results indicate that nitrogen is buried below PEG and hence XPS signals in PEG-coated samples indicate more of PEG nano layer coated above CS/TPP nanoparticles. Surface composition in terms of O/N and C/N atomic ratios of PEG-coated CS/TPP nanoparticles and CS/TPP nanoparticles is given in Table I. High resolution C (1S) spectra of PEG, PEG-coated CS/TPP nanoparticles and CS shown in Figure 10(B) show presence of C—C and C—H functionality at 285.0 ± 0.1 eV[57] and C—O—C, C—OH, and

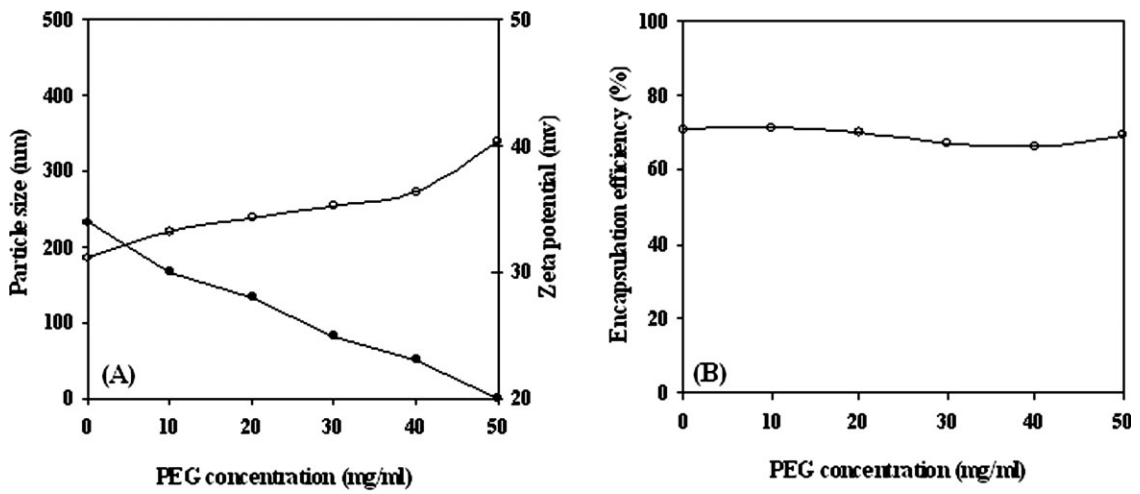

Figure 8 Effect of PEG concentrations on (A) particle size (○), zeta potential (●), and (B) encapsulation efficiency of VHL in CS nanoparticles. (CS/TPP mass ratio 5 : 1, venlafaxine hydrochloride = 0.6 mg/mL, pH = 5).

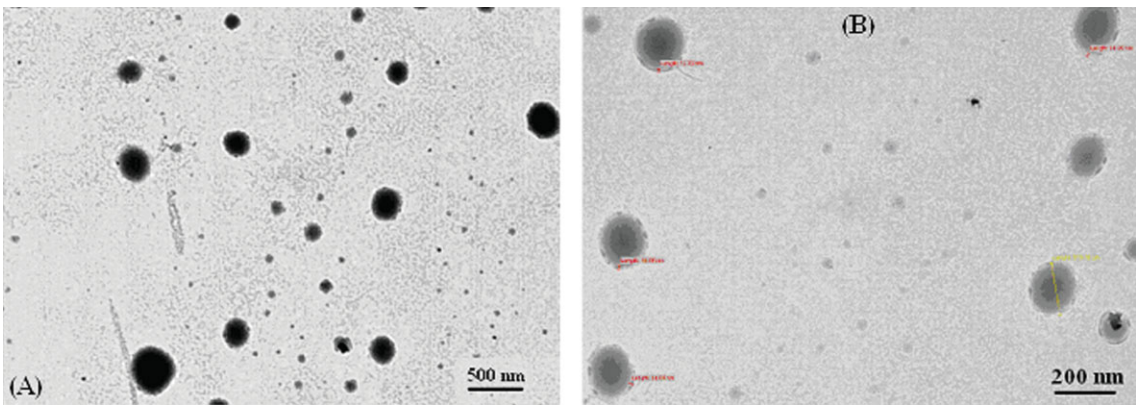

Figure 9 TEM image of (A, B) PEG-coated CS/TPP nanoparticles. (CS/TPP mass ratio = 5 : 1, VHL = 0.6 mg/mL, PEG = 30 mg/mL and pH = 5). [Color figure can be viewed in the online issue, which is available at www.interscience.wiley.com.]

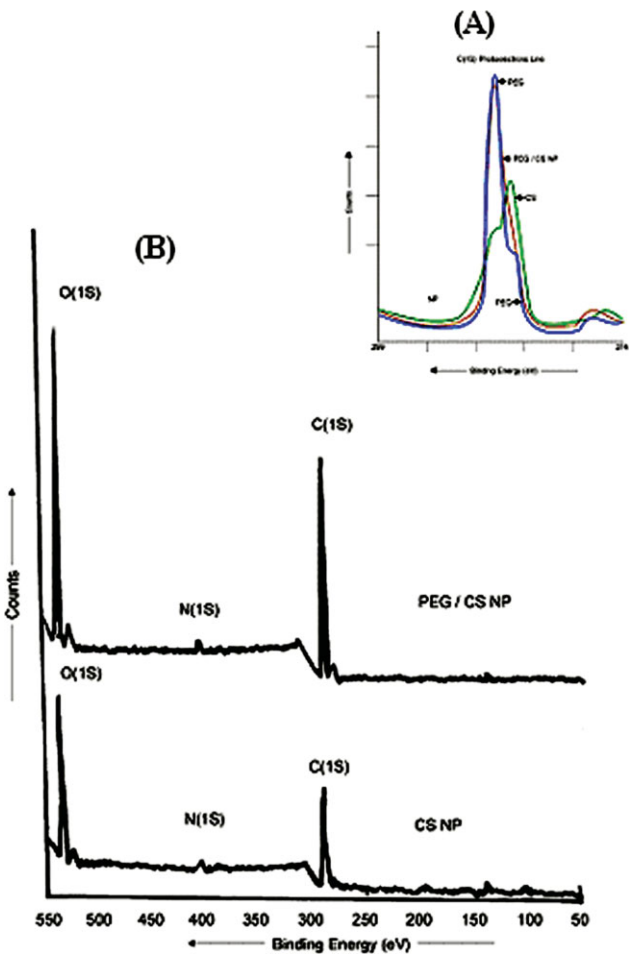

Figure 10 XPS analysis of CS, PEG, CS/TPP and PEG-coated CS/TPP nanoparticles. (A) High resolution C (1S) photoelectron line showing carbon functionalities and relative composition in CS, PEG, and PEG-coated CS nanoparticles and (B) XPS survey scan of CS/TPP nanoparticles and PEG-coated CS/TPP nanoparticles. [Color figure can be viewed in the online issue, which is available at www.interscience.wiley.com.]

C—N functionalities[58,59] at 286.6 ± 0.1 eV. It is worth mentioning that N (1S) spectra shape shown in quantitative data is broad because these functionalities are not resolved properly in low resolution data. Thus XPS data shown in Figure 10(A,B) indicate that although nitrogen signal is very small, it is visible in PEG-coated CS/TPP nanoparticles layer. This suggests that CS/TPP nanoparticles are coated with monolayer of PEG as it is also seen in TEM picture [Fig. 9(A,B)].

In vitro release study

Figure 11(A) shows the release profile of VHL from CS and PEG-coated CS/TPP nanoparticles. It was observed from the plots that, *in vitro* release of VHL shows a very rapid initial burst followed by a slow drug release at 7.4 pH. Generally the drug release is due to the diffusion of drug molecules through the matrix or due to degradation of polymeric matrix. In the present case, initial burst release of drug molecules from nanoparticles can be attributed to the presence of drug molecules near the periphery of the nanoparticles, which diffuse in the surrounding medium due to rapid penetration of release medium in the hydrophilic nanoparticles. The release rate was observed to be slow for PEG-coated CS/TPP nanoparticles as compared to unmodified nanoparticles due to the presence of surface crosslinking of PEG [Fig. 9(B)], which produces hindrance to the diffusion of drug molecules in release medium. Figure 11(B–D) shows the effect of drug, CS concentration and CS/TPP mass ratio on release of the drug respectively. It was observed that, with increase in the initial drug concentration in the nanoparticles, its release rate is also observed to increase upto 600 μg/mL and there after release rate is observed to decrease. This can be attributed to the

TABLE I
XPS Composition of CS/TPP Nanoparticles and PEG-Coated CS/TPP Nanoparticles

Sample	C (Atomic %)	N (Atomic %)	O (Atomic %)	C/N (Atomic ratio)	O/N (Atomic ratio)
CS nanopatticles	63.2	6.2	30.6	10.2	4.9
PEG-coated CS nanoparticles	67.1	1.7	31.2	39.5	18.4

observed maximum encapsulation efficiency of VHL at 600 μg/mL concentration [Fig. 7(A)]. As encapsulation efficiency decreases after 600 μg/mL drug concentration it directly affects the release rate. Total cumulative release was observed to reduce from 90 to 56% when the CS concentration increased from 0.5 to 2.5 mg/mL [Fig. 11(C)]. This can be attributed to the increased viscosity of the solution, hindering the ionic interaction between CS and TPP resulting in less compact nanoparticle matrix and hence subsequently low encapsulation and release rate. Similar results are also reported by Gan and Wang.[45] Figure 11(D) shows the effect of CS/TPP mass ratio on the release profile. It was observed that when CS/TPP mass ratio decreases from 7 to 3, total cumulative release increases from 78 to 97%. Hence, at low CS/TPP mass ratio, faster release rate is observed as compared to higher CS/TPP mass ratio. The % relative error calculated for triplicate measurements was observed to be less than 6.2%.

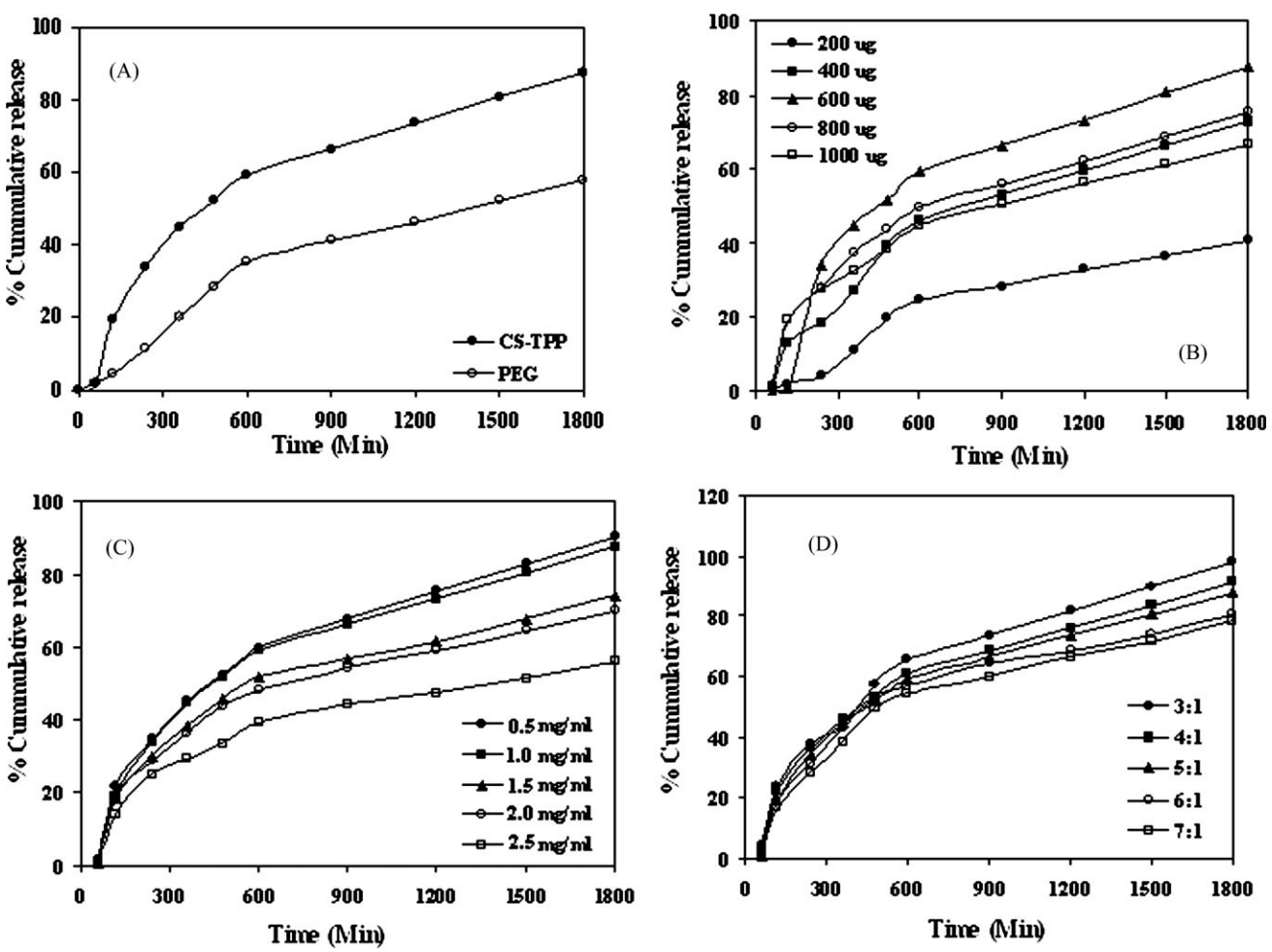

Figure 11 *In vitro* release profile of VHL from CS/TPP nanoparticles. (A) *In vitro* release of VHL from (●) CS/TPP nanoparticles and (○) PEG-coated CS/TPP nanoparticles synthesized at CS/TPP mass ratio 5 : 1. CS, PEG and VHL concentrations 1.5 mg/mL, 30 mg/mL, 600 μg/mL, respectively. (B) Effect of VHL concentration on the % cumulative release from CS/TPP nanoparticles synthesized at CS/TPP mass ratio: 5 : 1and pH = 5. (C) Effect of CS concentration on the % cumulative release from CS/TPP nanoparticles synthesized at CS/TPP mass ratio: 5 : 1 and pH = 5. (D) Effect of CS/TPP mass ratio on the % cumulative release from CS/TPP nanoparticles. Concentration of CS and VHL = 1.5 mg/mL and 0.6 mg/mL.

CONCLUSIONS

The CS/TPP nanoparticles and PEG-coated CS/TPP nanoparticles can be formed under very mild experimental conditions. Physiochemical properties such as particle size and zeta potentials can be simply manipulated and controlled by varying the key processing parameters such as CS, PEG concentration and CS/TPP mass ratio. Molecular level dispersion of VHL within the nanoparticles was observed from XRD and DSC analysis. Entrapment efficiency up to (70 ± 5)% was observed for CS/TPP nanoparticles at 0.6 mg/mL drug concentration. However, manipulation of these conditions did not succeed in controlling the burst release of encapsulated drug. Addition of PEG during nanoparticle formation has no effect on encapsulation efficiency of drug but shows decrease in zeta potential, increase in particles size and stability of nanoparticles with delayed release of entrapped drug molecules due to increased bulk density and coating as observed in TEM on the nanoparticles. XPS investigation also reveals the presence of PEG on the surface of CS/TPP nanoparticles, a fact that renders them interesting carrier for drug delivery applications.

References

1. Illum, L. Pharm Res 1998, 15, 1326.
2. Illum, L. J Pharm Sci 2007, 96, 473.
3. Ngah, W. S. W.; Ghani, S. Ab.; Kamari, A. Bioresource Technol 2005, 96, 443.
4. Gumusderelioglu, M.; Agi, P. React Funct Polym 2004, 61, 211.
5. Nakajima, M.; Atsumi, K.; Kifune, K. In Development of Absorbable Sutures from Chitosan and Related Enzymes; Harcourt Brace Janovich: New York, 1984.
6. Douglas, B. D.; Odilio, A.; De, B. G. Int J Biomacromol 2007, 41, 198.
7. Rinaudo, M. Prog Polym Sci 2006, 31, 603.
8. Wang, Y. L.; Gu, H. Y.; Su, Z. G.; Ma, H. G. Int J Pharm 2006, 311, 187.
9. Tozaki, H.; Komoike, J.; Tada, C.; Maruyama, T.; Terabe, A.; Suzuki, T.; Yamamoto, A.; Muranishi, S. J Pharm Sci 1997, 86, 1016.
10. Liu, Z. D.; Sheu, T. M.; Chen, H. C.; Yang, R. Y.; Ho, O. H. J Controlled Release 2007, 118, 333.
11. Kristl, J.; Smid-Korbar, J.; Strue, E.; Schara, M.; Rupprecht, H. Int J Pharm 1993, 99, 13.
12. Portero, A.; Teijeiro-Osorio, D.; Alonso, M. J.; Remuñán-López, C. Carbohydr Polym 2007, 68, 617.
13. Takeuchi, H.; Yamamoto, H.; Niwa, T.; Hino, T.; Kawashima, Y. Pharm Res 1996, 13, 896.
14. Lavelle, E. Exp Opin Ther Pat 2000, 10, 179.
15. Vander lubben, I. M.; Verhoef, J. C.; Barchard, G.; Junginer, H. E. Adv Drug Delivery Rev 2001, 52, 139.
16. Papadimitriou, S.; Bikiaris, D.; Avgoustakis, K.; Karavas, E.; Georgarakis, M. Carbohydr Polym 2008, 73, 44.
17. Shu, X. Z.; Zhu, K. J.; Song, W. Int J Pharm 2001, 212, 19.
18. Brigger, I.; Morizet, J.; Albert, G.; Chacun, H.; Ferrier-Lacombe, M. J.; Couverer, P.; Vassal, G. J. J Pharmacol Exp Ther 2002, 303, 928.
19. Thanoo, B. C.; Sunny, M. C.; Jaykrishnan, A. J Pharm Pharmacol 1992, 44, 283.
20. Genta, I.; Castantini, M.; Asti, A.; Conti, B.; Montanari, L. Carbohydr Polym 1998, 36, 81.
21. Pan, Y.; Li, Y. J.; Zhao, H. Y.; Zhang, J. M.; Xu, H.; Wei, G.; Hao, J. S.; Cui, F. D. Int J Pharm 2002, 249, 139.
22. Berger, J.; Reist, M.; Mayer, J. M.; Felt, O.; Peppas, N. A.; Gurny, R. Eur J Pharm Biopharm 2004, 57, 19.
23. Ko, J. A.; Park, H. J.; Hmang, S. J.; Park, J. B.; Lee, J. S. Int J Pharm 1997, 152, 37.
24. Genta, I.; Perugini, P.; Canti, B.; Pavenetto, F. Int J Pharm 1997, 152, 237.
25. He, P.; Davis, S. S.; Illum, L. Int J Pharm 1999, 187, 53.
26. Bayomi, M. A.; Al-Suwajeh, S. A.; El-Helw, A. M.; Masnad, A. F. Pharm Acta Helv 1998, 73, 187.
27. Jenes, K. A.; Fresneau, M. P.; Marazuela, A.; Fabra, A.; Alonso, M. J. J Controlled Release 2001, 73, 255.
28. Badmeier, R.; Chen, H.; Paeratakulm, O. Pharm Res 1989, 6, 413.
29. Desai, M. P.; Labhasetwar, V.; Walter, E.; Levy, R. J.; Amidom, G. L. Pharm Res 1997, 14, 1568.
30. Gref, R.; Minamitake, Y.; Perracchia, M. T.; Treubeskoy, V.; Torchilin, V.; Langer, R. Science 1994, 263, 1600.
31. Zhang, X.; Zhang, H.; Wu, Z.; Wang, Z.; Niu, H.; Li, C. Eur J Pharm Biopharm 2008, 68, 526.
32. Calvo, P.; Remunan-Lopez, C.; Vila-Jato, J. L.; Alonso, M. J. J Appl Polym Sci 1997, 63, 125.
33. Wu, Y.; Yang, W.; Wang, C.; Hu, J.; Fu, S. Int J Pharm 2005, 295, 235.
34. Gupta, K. C.; Ravikumar, M. N. V. J Mater Sci Mater Med 2001, 12, 753.
35. Sugimopto, M.; Morimoto, M.; Sashima, H.; Shigemusa, Y. Carbohydr Polym 1998, 36, 49.
36. Mo, X.; Aiba, S.; Wang, P.; Hayashi, K.; Xu, Z. In Advances in Chitin Science; Domard, A.; Robert, G. A. F.; Varum, K. M., Eds.; Andre: Lyon, 1998; vol. II, p 396.
37. Tokora, S.; Sekiguchi, H.; Takahashi, K.; Douba, K.; Sakairi, N.; Nishi, N.; Heta, K.; Satake, M. In Advances in Chitin Science; Domard, A.; Robert, G. A. F.; Varum, K. M., Eds.; Andre: Lyon, 1998; vol. II, p 608.
38. Klamerus, K. J.; Maloney, K.; Rudolph, R. L.; Sisenwine, S. F.; Jusko, W. J.; Chiang, S. T. J Clin Pharmacol 1992, 32, 716.
39. Burnett, F. E.; Dinan, T. G.; Hum Psychopharma 1998, 13, 169.
40. Yang, H.; Lopina, S. T. J Biomed Mater Res 2005, 72, 107.
41. Kere, J.; Ljubljana, T.; Humar, V.; Stahavica, G. WO Pat. WO 03/055475 A1, p 1–32.
42. Sherman, D. M.; Clark, J. C.; Lamer, J. U.; White, S. A. U.S. Pat. 6,419,958, p 1–30.
43. Kaushik, V. K. J Electron Spectrosc 1991, 56, 273.
44. Hu, Y.; Jiang, X.; Ding, Y.; Ge, H.; Yuan, Y.; Yang, C. Biomaterials 2002, 23, 3193.
45. Gan, Q.; Wang, T. Colloids Surf B 2007, 59, 24.
46. Sun, Y.; Wan, A. J Appl Polym Sci 2007, 105, 552.
47. Lin, Y. H.; Mi, F. L.; Chen, C. T.; Chang, W. C.; Peng, S. F.; Liang, H. F.; Sung, H. W. Biomacromolecule 2007, 8, 146.
48. Singla, A. K.; Chawla, D. M.; Biotech Histochem 2003, 78, 243.
49. Wan, Y.; Creber, K. A. M.; Peppley, B.; Bui, V. T. Macromol Chem Phys 2003, 204, 850.
50. Sarmento, B.; Ferreira, D.; Veiga, D.; Antonio, R. Carbohydr Polym 2006, 66, 1.
51. Panyam, J.; Labhasetwar, V. Adv Drug Delivery Rev 2003, 55, 329.
52. Gaserod, O.; Jolliffe, A. G.; Hampson, F. C.; Dettmar, P. W. S.; Kjak-Braek, G. Int J Pharm 1998, 175, 237.
53. Smith, J.; Wood, E.; Dornish, M. Pharm Res 2004, 21, 43.
54. Panyam, J.; Zhou, W. Z.; Prabha, S.; Sahoo, S. K.; Labhasetwar, V. FASEB J 2002, 16, 1217.
55. Mi, F. L.; Shyu, S. S.; Lee, S. T.; Wong, T. B. J Appl Polym Sci 37, 14, 1551.
56. Hu, Y.; Jiang, X.; Ding, Y.; Ge, H.; Yuan, Y.; Yang, C. Biomaterials 2002, 23, 319.
57. Yu, Y.; Li, W.,Yu, T. Polym Commun 1991, 31, 319.
58. Kaushik, V. K.; Bhardwaj, A. Polymer 1994, 13, 355.
59. Kaushik, V. K. Polym Test 2000, 19, 17.